Aaron L. Sverdlov, Aly Elezaby, Jessica B. Behring, Markus M. Bachschmid, Ivan Luptak, Vivian H. Tu, Deborah A. Siwik, Edward J. Miller, Marc Liesa, Orian S. Shirihai, David R. Pimentel, Richard A. Cohen, Wilson S. Colucci

High fat, high sucrose diet causes cardiac mitochondrial dysfunction due in part to oxidative post-translational modification of mitochondrial complex II

Journal of Molecular and Cellular Cardiology, 2015; 78:165-173

Originally published at: http://dx.doi.org/10.1016/j.yjmcc.2014.07.018

High fat, high sucrose diet causes cardiac mitochondrial dysfunction due in part to oxidative post-translational modification of mitochondrial complex II

Aaron L. Sverdlov[a], MBBS, PhD; Aly Elezaby[a], BS; Jessica B. Behring[b], BS; Markus M. Bachschmid[b], PhD; Ivan Luptak[a], MD, PhD; Vivian H. Tu[a], BS; Deborah A. Siwik[a], PhD; Edward J Miller[a], MD, PhD; Marc Liesa[c], PhD; Orian S Shirihai[c], MD, PhD; David R. Pimentel[a], MD; Richard A. Cohen[b], MD; Wilson S. Colucci[a], MD

[a] Myocardial Biology Unit, Boston University School of Medicine, Boston, MA

[b] Vascular Biology Unit, Boston University School of Medicine, Boston, MA

[c] Obesity and Nutrition Section, Mitochondria ARC, Boston University School of Medicine, Boston, MA

Corresponding author: Wilson S. Colucci, M.D.

Cardiovascular Medicine Section

Boston University Medical Center

88 E Newton St, Boston, MA 02118.

Tel: 617-638-8706

E-mail: wilson.colucci@bmc.org

Abstract

Background: Diet-induced obesity leads to metabolic heart disease (MHD) characterized by increased oxidative stress that may cause oxidative post-translational modifications (OPTM) of cardiac mitochondrial proteins. The functional consequences of OPTM of cardiac mitochondrial proteins in MHD are unknown. Our objective was to determine whether cardiac mitochondrial dysfunction in MHD due to diet-induced obesity is associated with cysteine OPTM.

Methods and results: Male C57Bl/6J mice were fed either a high-fat, high-sucrose (HFHS) or control diet for 8 months. Cardiac mitochondria from HFHS-fed mice (vs. control diet) had an increased rate of H_2O_2 production, a decreased GSH/GSSG ratio, a decreased rate of complex II substrate-driven ATP synthesis and decreased complex II activity. Complex II substrate-driven ATP synthesis and complex II activity were partially restored *ex-vivo* by reducing conditions. A biotin switch assay showed that HFHS feeding increased cysteine OPTM in complex II subunits A (SDHA) and B (SDHB). Using iodo-TMT multiplex tags we found that HFHS feeding is associated with reversible oxidation of cysteines 89 and 231 in SDHA, and 100, 103 and 115 in SDHB.

Conclusions: MHD due to consumption of a HFHS "Western" diet causes increased H_2O_2 production and oxidative stress in cardiac mitochondria associated with decreased ATP synthesis and decreased complex II activity. Impaired complex II activity and ATP production are associated with reversible cysteine OPTM of complex II. Possible sites of reversible cysteine OPTM in SDHA and SDHB were identified by iodo-TMT tag labeling. Mitochondrial ROS may contribute to the pathophysiology of MHD by impairing the function of complex II.

Keywords: metabolic heart disease, obesity, mitochondria, oxidative stress, oxidative protein modifications

Abbreviations

BIAM - biotin-iodoacetamide

DTT – dithiothreitol

GSH/GSSG – ratio of reduced to oxidized glutathione

HFHS - high fat / high sucrose

MHD – metabolic heart disease

OPTM - oxidative post-translational modifications

ROS – reactive oxygen species

SDH – succinate dehydrogenase

SDHA - succinate dehydrogenase subunit A

SDHB - succinate dehydrogenase subunit B

SDHC - succinate dehydrogenase subunit C

SDHD - succinate dehydrogenase subunit D

1. Introduction

Obesity-related metabolic syndrome increases the risk for metabolic heart disease (MHD), a common cardiomyopathy characterized by impaired energetics [1, 2] and myocardial dysfunction [3]. The mechanism responsible for impaired energetics in MHD is not understood. Another potentially important feature of MHD is increased ROS production within the mitochondria [1, 4]. While the role of mitochondrial ROS in the pathophysiology of MHD is not known [5], it is increasingly evident that elevated levels of ROS can adversely affect cell function by causing oxidative post-translational modifications (OPTM) that regulate protein activity [6]. Relatively little is known about OPTM of mitochondrial proteins [7], and no prior study has assessed the functional consequences of cardiac mitochondrial protein OPTM in MHD.

We recently described the cardiac phenotype in a mouse model of metabolic syndrome induced by a "Western-style", high fat / high sucrose (HFHS) diet [3]. In these mice HFHS feeding causes MHD with diastolic dysfunction and elevated oxidative stress in the myocardium - both of which are ameliorated by antioxidant therapy [3]. In a preliminary assessment of cysteine OPTM using iodo-TMT multiplex tags we found that HFHS feeding is associated with reversible OPTM of cysteines in several cardiac mitochondrial proteins [8]. Together these observations raised the possibility that impaired energetic function in MHD is due to OPTM of mitochondrial proteins. Accordingly, the goal of this study was to test the hypothesis that impaired ATP synthesis in HFHS-fed mice is due to reversible cysteine OPTM of one or more mitochondrial proteins. As a first approach we evaluated the effect of HFHS feeding on mitochondrial function by measuring mitochondrial ATP production, ROS generation, electron transport chain complex function, and the ability of a reducing environment to restore function. We then used the results of the functional analysis to direct the assessment of reversible OPTM

using a biotin switch assay and targeted analysis of a dataset in which reversible cysteine OPTM were labeled with iodo-TMT multiplex tags [8].

2. Methods

2.1. Experimental animals. Male C57BL/6J mice 9 weeks of age were fed *ad libitum* either a control chow diet (Research Diets, product No. D09071703, 10% kcal lard, 0% sucrose) or a HFHS diet (Research Diets, product No. D09071702; 58% kcal lard, 13% kcal sucrose) for 8 months. Diets were matched for caloric value and full composition is provided in **Table S1**. By two months on diet, HFHS-fed mice weighted more than CD-fed mice and the degree of obesity increased progressively over time through 8 months (**Figure 1S**). The protocol was approved by the Institutional Animal Care and Use Committee at Boston University School of Medicine.

2.2. Mitochondrial isolation. Heart mitochondria were essentially isolated as previously described by us with minor modifications [9]. All steps were performed at 4ºC. Briefly, tissues were rinsed in a buffer containing 100 mM KCl, 5 mM EGTA and 5 mM HEPES at pH 7.0, and thereafter homogenized in 2 ml of HES buffer (HEPES 5 mM, EDTA 1 mM, Sucrose 0.25M, pH 7.4 adjusted with KOH 1M) using a Teflon-on-glass electric homogenizer. The homogenate was centrifuged at 500 × g for 10 minutes at 4 °C. The supernatant was then centrifuged at 9000 × g for 15 minutes at 4ºC and the mitochondrial pellet was resuspended in 100-200 µl of HES buffer with 0.2% of BSA fatty acid-free. Protein was quantified using BCA (Pierce) and the value of HES-BSA buffer alone was subtracted.

2.3. Mitochondrial H_2O_2 production. Mitochondrial H_2O_2 production was measured using the Amplex Ultra Red-Horseradish peroxidase method (Invitrogen) as described previously with minor modifications [10]. This assay is based on the Horseradish peroxidase (2 units/ml)

H_2O_2-dependent oxidation of nonfluorescent Amplex Ultra Red (50 μM) to fluorescent resorufin red. In short, 10 μg mitochondria were diluted in 50 μl reaction buffer (125 mM KCl, 10 mM HEPES, 5 mM $MgCl_2$, 2 mM K_2HPO_4, pH 7.44) to determine complex I (pyruvate /malate, 5 mM) or complex II (succinate, 5 mM) driven H_2O_2 production with and without inhibitors (rotenone 2μM, antimycin A, 0.5μM). Mitochondrial H_2O_2 production was measured after the addition of 50 μl of reaction buffer containing horseradish peroxidase and Amplex Ultra Red. Fluorescence was followed at an excitation wavelength of 545 nm and an emission wavelength of 590 nm for 20 minutes. The assay is performed in a 96-well plate using a Tecan M1000 plate reader. The plate is set up so that all experimental conditions for each animal, as well as a standard curve for each run, are acquired and monitored over time simultaneously in duplicate. The slope of the increase in fluorescence is converted to the rate of H_2O_2 production with a standard curve. All of the assays were performed at 25 °C. The results are reported as pmoles/min/mg protein.

2.4. Mitochondrial reduced (GSH) and oxidized (GSSG) glutathione measurements.

Reduced and oxidized glutathione were simultaneously measured as previously described with minor modifications [11, 12]. Briefly, mitochondria were lysed in the presence of iodoacetic acid (10mM) and derivatized with fluorescent dansyl chloride. Derivatized samples were separated and analyzed with hydrophilic interaction liquid chromatography on a Restek Ultra Amino 3um 100x3.2mm HPLC column at a flow rate of 0.6 ml/min. Buffer A (80% methanol, 20% water) was changed in a linear gradient to 30% of buffer B (acetate-buffered (pH 4.6) methanol solution) to elute reduced and oxidized glutathione with a Varian ProStar 230 HPLC system. Fluorescent products were detected with a Shimadzu RF-10A_{XL} set to 335nm for excitation and 541nm for emission.

2.5. ATP production in isolated mitochondria. ATP synthesis rates in isolated heart mitochondria were determined using the luciferin/luciferase based ATP Bioluminescence Assay Kit CLS II (Roche) with minor modifications [13]. In short, 10 μg of heart mitochondria were suspended in 75 μl buffer A (125 KCl, 10mM Hepes, 5 mM $MgCl_2$ and 2 mM K_2HPO_4, pH7.44) to determine complex I (pyruvate/ malate, 5mM final) or complex II (succinate, 5 mM final) driven ATP synthesis. Following standard practice, succinate driven ATP generation was measured in the presence of complex I inhibitor rotenone (0.5μM) to avoid the reverse electron transfer effect [14]. The assays were performed in the presence and absence of Dithiothreitol (DTT, 5mM). Measurements with substrates were repeated in the presence of inhibitors of respiratory complex (rotenone (CI) and oligomycin (C IV) to determine the rates of non-mitochondrial ATP production. The background of the assay was determined with mitochondria alone. The measurements for all samples were started simultaneously by adding 75 μl of luciferin/luciferase buffer containing 1mM ADP (0.5mM final). The initial slope of the increase in ATP-supported luciferase chemiluminescence was used to determine the rate of ATP production after subtraction of the background and non-mitochondrial values. Using an ATP standard provided in the kit, the slopes were converted in nmoles/min/mg protein.

***2.6. Mitochondrial ETC complex II activity*.** Complex II enzyme activity of isolated mitochondria was measured using microplate assay kit (Abcam/Mitosciences ab109908/MS241), as previously described [15]. In this assay kit, complex II is immunocaptured within the wells of the microplate. The production of ubiquinol by complex II is coupled to the reduction of the dye DCPIP (2,6-diclorophenolindophenol) and a decreases in its absorbance at 600 nm is measured spectrophotometrically. The assay is performed in the presence of succinate as a substrate. The

assay was performed in the presence and absence of 5mM DTT. Enzymatic activity was normalized to mitochondrial protein concentration.

2.7. Immunoblotting for mitochondrial proteins. Immunoblots were performed on frozen LV that was homogenized in tissue lysis buffer (HEPES, pH 7.4, 20 mmol/L, B-glycerol phosphate 50 mmol/L, EGTA 2 mmol/L, dithiothreitol 1 mmol/L, NaF 10 mmol/L, $NaVO_4$ 1 mmol/L, Triton X-100 1%, glycerol 10%, and 1 protease inhibitor complete mini tablet, EDTA free, 20 mL [Roche]). Total protein (25 μg) was separated by sodium dodecyl sulfate polyacrylamide gel electrophoresis and transferred to polyvinylidene fluoride membranes. Blots were incubated with mouse total OXPHOS Rodent WB Antibody cocktail [containing 5 antibodies, one each against complex I subunit NDUFB8, complex II subunit B (SDHB), complex III Core protein 2 (UQCRC2), complex IV subunit I (MTCO1) and CV alpha subunit (ATP5A)] (Abcam, MA, USA; ab110413), anti-SDHA, SDHB, SDHC (Abcam, MA, USA; ab14715, ab14714 and ab155999 respectively) and SDHD (Thermo Fisher; PA5-34387) antibodies, anti-VDAC1 (Abcam, MA, USA; ab15895) and anti-GAPDH (Abcam, MA, USA; ab8245) and detected with the use of the Licor Odyssey two-color infrared imaging system.

2.8. Biotin switch assay. Labeling with biotin iodoacetamide (BIAM; Life Technologies; B-1591) was used in a biotin switch assay to detect reversibly oxidized cysteines, as previously described by us [16] with minor modifications. Freshly isolated LV sections were immediately snap-frozen and stored in liquid nitrogen. Tissue was thawed and lysed in RIPA buffer containing 100 mM maleimide (NEM) to block all free thiols and prevent further oxidation. Excess NEM was removed by passing the lysates over Zeba™ spin columns. NEM-labeled proteins are treated with 5 mM DTT at room temperature for 15 minutes to reduce reversible oxidations to free thiols, and again column cleaned to eliminate DTT. Samples are incubated

with 4 mM BIAM for 2 hours at room temperature in the dark, labeling any reactive free thiols that were previously oxidized. BIAM-labeled proteins are gathered from total protein with streptavidin magnetic beads (50 µL) for 1 hour at room temperature in the dark, washed, and cleaved from beads by boiling in 30 ml of 2× non-reducing Laemmli buffer for 10min. BIAM-labeled and unlabelled complex II proteins are detected by western blotting with anti-SDHA, SDHB, SDHC (Abcam) and SDHD (Thermo Fisher) antibodies, and bands detected by near-infrared dye-conjugated secondary antibodies and quantified with the Licor Odyssey two-color infrared imaging system. Ratio of labeled to unlabeled proteins represents percentage reversibly oxidized cysteines in each specific subunit.

2.9. Iodo-TMT multiplex tag labeling of cysteines. We analyzed a dataset previously acquired in this model [8] to quantify relative changes in reversible OPTM of complex II cysteines. Briefly, proteomic and Thermo iodo-TMT technology was used to differentially-label reversibly oxidized and total available cysteines in the left ventricle of HFHS-fed mice. The data analysis using Proteome Discoverer (PD) was performed as described [8], with the following modification: Direct measurement of the expression of complex II subunits by immunoblotting allowed the use of the raw ion intensity sums for reporter ions *m/z* 129 and 127, which indicate HFHS OPTM and CD OPTM respectively, to generate the relative fold-change in reversible oxidation.

2.10. Statistical analysis. Results are presented as mean±SEM. Comparisons between groups were performed using unpaired t-tests, Mann-Whitney non-parametric tests or 2-way ANOVA as appropriate. All statistical analyses were performed using GraphPad Prism version 6 software. P-value < 0.05 was considered statistically significant.

3. Results

3.1. HFHS diet increases mitochondrial ROS production. In cardiac mitochondria from HFHS-fed mice H_2O_2 production was increased with complex I or II substrates (**Figure 1A and 1B**). The cardiac mitochondrial GSH/GSSG ratio was decreased in HFHS-fed mice confirming an increase in mitochondrial oxidative stress (**Figure 1C**). The total myocardial GSH/GSSG ratio was likewise decreased in HFHS-fed animals (**Figure 1D**).

3.2. HFHS diet impairs mitochondrial ATP synthesis. In mitochondria from HFHS-fed mice ATP synthesis rate was decreased for complex I or II substrates (**Figure 2A and 2B**). In mitochondria from HFHS-fed mice pre-incubation with DTT (5mM) had a minimal effect on complex I substrate-driven ATP synthesis (~ 11% increase; p=0.13), but caused a ~33% increase with complex II substrate (p=0.01 vs. control diet; p = 0.02 vs. complex I substrate) (**Figure 2A and 2B**). HFHS feeding had no effect on the expression of electron transport complex (ETC) subunits or VDAC-1 (Figure **4**).

3.3. HFHS diet decreases complex II activity. Complex II (succinate dehydrogenase, SDH) activity was decreased by ~70% in mitochondria from HFHS-fed mice (**Figure 2C**). As with ATP production rate, DTT (5mM) caused a partial recovery of complex II activity in HFHS-fed mice, though not to the levels observed in control diet-fed mice.

3.4. HFHS diet causes reversible cysteine OPTM in complex II proteins. To determine whether there is reversible cysteine oxidation in complex II proteins, we performed a biotin-switch assay in which free thiols are blocked with *N*-Ethylmaleimide - reversibly oxidized thiols are then reduced with DTT (as per the ATP and complex II activity assays), labeled with biotin-iodoacetamide (BIAM) and immunoblotted for complex II subunit proteins. HFHS feeding increased the quantity of reversibly-oxidized thiols in SDH subunits A and B (**Figure 3**).

Subunits C and D could not be resolved sufficiently to allow quantitation. However, neither was identified as differentially-modified by iodo-TMT/MS.

Based on the identification of SDHA and SDHB as sites of reversible cysteine OPTM we re-interrogated a proteomics dataset of reversible cysteine OPTM in this model [8] specifically focusing on complex II subunits. We found that protein expression of SDHA and SDHB assessed by immunoblotting was unchanged (**Figure 4**), which allowed us to utilize the ratio of reversibly-oxidized cysteines between CD and HFHS-fed mice to identify those that are differentially oxidized in complex II (**Figure 5**). This approach is modified from that published by our group [8] where relative protein expression was based on the total available cysteines tagged by iodo-TMT, rather than actual protein expression. By measuring total protein expression, rather than total available cysteines, we increased the accuracy of protein determination by discounting the potentially confounding effect of conformational changes and irreversible cysteine modifications in these proteins (**Table 1**). Consistent with the biotin switch data, SDHA and SDHB were subject to differential oxidative modifications. In SDHA, Cys89 and Cys231 OPTM were increased 1.94- and 2.14-fold, respectively in HFHS-fed mice. In SDHB, Cys100, Cys103 and Cys115 OPTM were increased 1.43-fold in HFHS-fed mice.

4. Discussion

The major new findings of this study are that diet-induced MHD is associated with a) increased mitochondrial production of H_2O_2 and oxidative stress, b) decreased complex I and II-driven ATP synthesis, c) markedly decreased complex II activity, d) partial rescue of both complex II substrate-driven ATP synthesis and complex II activity by a reducing environment, and e) reversible cysteine OPTM of complex II subunits SDHA and SDHB. Together these

observations provide the first demonstration of reversible cysteine OPTM that are associated with mitochondrial dysfunction in MHD.

4.1. Impaired mitochondrial ATP synthesis and complex II activity. HFHS feeding was associated with decreased ATP synthesis driven by complex I or II substrates. This finding is consistent with observations in both humans and animals with obesity. In obese humans myocardial energetics assessed by measurement of high energy phosphates using ^{31}P NMR are impaired [17] and improve with weight loss [18]. Likewise, studies in *ob/ob* and *db/db* mice show decreased cardiac mitochondrial ATP synthesis [1, 4].

Complex II substrate-driven ATP synthesis was decreased in HFHS-fed mice. Complex II couples the oxidation of succinate to fumarate in the matrix with the reduction of ubiquinone in the membrane [19]. To assess complex II activity directly we measured the production of ubiquinol [15], which demonstrated that HFHS feeding caused a marked decrease in complex II activity. Complex II consists of four nuclear-encoded proteins - SDH subunits A, B, C and D. SDHA and SDHB are exposed to the matrix, while SDHC and SDHD are in the inner membrane [20]. There was no decrease in the expression of SDHA, SDHB or SDHC with HFHS feeding, indicating that the observed decrease in function is not due to decreased protein expression. Likewise, HFHS feeding was not associated with decreases in representative proteins from complex I, III, IV or V; and was not associated with a decrease in mitochondrial mass as reflected by VDAC expression (**Figure 4**).

4.2. HFHS-induced cysteine OPTM of complex II. The ability of DTT to partially correct complex II substrate-driven ATP synthesis and complex II activity, in the absence of a change in complex II protein expression, suggests that the decrease in activity is mediated, at least in part, by reversible cysteine OPTM. A large number of proteins involved in cardiac

function are subject to cysteine OPTM with effects on function ranging from stimulation to inhibition [6, 21, 22], and there are several reactive cysteines in complex II that can be oxidized [23, 24].

Using the biotin switch assay, we found that HFHS feeding causes reversible cysteine OPTM of both SDHA and SDHB. Based on the finding that the expression of SDHA and SDHB is unchanged by HFHS feeding, it was possible to further analyze complex II OPTM in a database derived using iodo-TMT multiplex tags in HFHS-fed mice [8]. The previous global analysis of this dataset determined relative protein expression based on the total available cysteines tagged by iodo-TMT [8], which may be confounded by irreversible cysteine modifications or conformational changes that limit access to certain cysteines. Because the expression of these proteins was determined directly, rather than indirectly based on the total number of cysteine, the accuracy of iodo-TMT tag labeling for determination of complex II OPTM was increased. This analysis identified OPTM of Cys89 and Cys231 in SDHA, and Cys100, Cys103 and Cys115 in SDHB in HFHS-fed mice.

While we cannot determine which of the identified OPTM are responsible for decreased complex II activity, it is noteworthy that Cys100, 103 and 115 are components of the 2Fe-2S iron-sulfur cluster which is critical for enzyme activity. Mutations of these sites have been noted to lead to decreased enzyme activity in bacteria [25]. Chen *et al.* [24] showed that S-glutathiolation of rat SDHA at Cys90 (Cys89 in mouse proteome) increases activity whereas ischemia/reperfusion causes de-glutathiolation leading to decreased complex II activity. Since the HFHS feeding-associated cysteine OPTM that we observed is associated with decreased complex II activity, S-glutathiolation at Cys89 is not likely to be the cause of decreased complex II activity with HFHS feeding. Other cysteines of complex II are known to undergo OPTM with

unknown functional significance. For example, S-nitrosylation of SDHA Cys536 was observed under resting conditions, but not with severe oxidative stress due to ischemia/reperfusion [26], while SDHA Cys430 and SDHC Cys107 were S-nitrosylated in rat myocardium under basal conditions [27]. Since the HFHS-induced decrease in complex II activity was only partially reversible under reducing conditions, additional irreversible OPTM of cysteine may be present (e.g., sulfonylation) or OPTM of other amino acids not reducible by DTT occur in this model (e.g., lysine) [6].

We cannot determine the contribution of complex II OPTM to overall mitochondrial dysfunction, or the relative contribution of complex II to overall mitochondrial ATP synthesis. However, it appears that the effect of DTT to increase ATP production is relatively specific for complex II since it had little or no effect on complex I substrate-driven ATP production. Complex II substrate-driven ATP production requires complex V (ATP synthase) function, which can be inhibited by glutathiolation in the setting of chronic heart failure [22]. However, since DTT did not increase complex I substrate-mediated ATP production, which also requires complex V, it is unlikely that the effect of DTT is due to increased complex V activity.

Mitochondrial uncoupling was identified in *ob/ob and db/db* mice [1, 4], and uncoupling protein 3 appears to play a role in mitochondrial uncoupling in mice on high fat diet, though not in *ob/ob* mice [28]. While we cannot exclude a role for uncoupling in HFHS-fed mice, the decrease in ATP production we observed was reversible for complex II but not complex I substrate-driven synthesis, suggesting that uncoupling is unlikely to be the main mechanism responsible for impaired ATP synthesis in this setting.

4.3. Mitochondrial ROS production in HFHS-fed mice. HFHS diet was associated with increased H_2O_2 production with both complex I and II substrates. The precise mechanism

responsible for electron leakage is not clear, but has been ascribed to substrate excess and/or reduced activity of ETC [29], the latter potentially related to OPTM-mediated dysfunction of ETC proteins. The observed increase in mitochondrial H_2O_2 production is consistent with prior observations in diabetic *db/db* mice [1]. Since the assay was performed without the addition of exogenous SOD, it is possible that the observed rates under- or over-estimate the actual H_2O_2 production rate if there are group-specific changes in SOD activity. While the major sources of mitochondrial ROS are thought to be complexes I and III, recent evidence suggests that complex II may produce ROS in disease states [19, 29]. The potential importance of mitochondrial ROS in MHD is supported by the demonstration that transgenic expression of MnSOD was protective of myocyte function in diabetic mice [30].

4.4. Conclusions. The demonstration that complex II dysfunction in HFHS-fed mice is associated with reversible OPTM provides a potential specific mechanism by which mitochondrial ROS could contribute to myocardial dysfunction in MHD. We further identified 5 cysteines which are reversibly-modified by HFHS feeding, and which alone or in combination may be responsible for impaired ATP synthesis. These findings suggest that the pathophysiologic role of complex II inhibition [19] may extend to MHD. An implication of these findings is that cardiac dysfunction in MHD may be a consequence of an ROS-mediated impairment in energetics. For example, reduced function of sarcoplasmic reticulum Ca^{++} ATPase, an enzyme which is highly sensitive to a decrease in ATP, may contribute to diastolic dysfunction, a hallmark of MHD [31]. Together these observations suggest that efforts to decrease mitochondrial ROS and / or protect target cysteines from oxidation may be of value in the therapy of MHD.

Sources of Funding

Supported by NIH grants HL-064750 (WSC), HL031607 (RAC), and the NHLBI-sponsored Boston University Cardiovascular Proteomics Center (Contract No. N01-HV-28178, RAC and WSC). Dr Sverdlov is funded by a CJ Martin Fellowship from the National Health and Medical Research Council of Australia (APP1037603) and the Marjorie Hooper Overseas Fellowship from the Royal Australasian College of Physicians.

Disclosures

None.

5. References

[1] Boudina S, Sena S, Theobald H, Sheng X, Wright JJ, Hu XX, et al. Mitochondrial energetics in the heart in obesity-related diabetes: direct evidence for increased uncoupled respiration and activation of uncoupling proteins. Diabetes. 2007;56:2457-66.

[2] Rider OJ, Francis JM, Ali MK, Petersen SE, Robinson M, Robson MD, et al. Beneficial cardiovascular effects of bariatric surgical and dietary weight loss in obesity. J Am Coll Cardiol. 2009;54:718-26.

[3] Qin F, Siwik DA, Luptak I, Hou X, Wang L, Higuchi A, et al. The polyphenols resveratrol and S17834 prevent the structural and functional sequelae of diet-induced metabolic heart disease in mice. Circulation. 2012;125:1757-64, S1-6.

[4] Boudina S, Sena S, O'Neill BT, Tathireddy P, Young ME, Abel ED. Reduced mitochondrial oxidative capacity and increased mitochondrial uncoupling impair myocardial energetics in obesity. Circulation. 2005;112:2686-95.

[5] Rosca MG, Hoppel CL. Mitochondrial dysfunction in heart failure. Heart Fail Rev. 2013;18:607-22.

[6] Kumar V, Calamaras TD, Haeussler D, Colucci WS, Cohen RA, McComb ME, et al. Cardiovascular redox and ox stress proteomics. Antioxid Redox Signal. 2012;17:1528-59.

[7] Murphy MP. Mitochondrial thiols in antioxidant protection and redox signaling: distinct roles for glutathionylation and other thiol modifications. Antioxid Redox Signal. 2012;16:476-95.

[8] Behring JB, Kumar V, Whelan SA, Chauhan P, Siwik DA, Costello CE, et al. Does reversible cysteine oxidation link the Western diet to cardiac dysfunction? FASEB J. 2014;28:1975-87.

[9] Liesa M, Luptak I, Qin F, Hyde BB, Sahin E, Siwik DA, et al. Mitochondrial transporter ATP binding cassette mitochondrial erythroid is a novel gene required for cardiac recovery after ischemia/reperfusion. Circulation. 2011;124:806-13.

[10] Muller FL, Liu Y, Abdul-Ghani MA, Lustgarten MS, Bhattacharya A, Jang YC, et al. High rates of superoxide production in skeletal-muscle mitochondria respiring on both complex I- and complex II-linked substrates. Biochem J. 2008;409:491-9.

[11] Jones DP, Carlson JL, Samiec PS, Sternberg P, Jr., Mody VC, Jr., Reed RL, et al. Glutathione measurement in human plasma. Evaluation of sample collection, storage and derivatization conditions for analysis of dansyl derivatives by HPLC. Clin Chim Acta. 1998;275:175-84.

[12] Reed DJ, Babson JR, Beatty PW, Brodie AE, Ellis WW, Potter DW. High-performance liquid chromatography analysis of nanomole levels of glutathione, glutathione disulfide, and related thiols and disulfides. Anal Biochem. 1980;106:55-62.

[13] Mansouri A, Muller FL, Liu Y, Ng R, Faulkner J, Hamilton M, et al. Alterations in mitochondrial function, hydrogen peroxide release and oxidative damage in mouse hind-limb skeletal muscle during aging. Mech Ageing Dev. 2006;127:298-306.

[14] Sahin E, Colla S, Liesa M, Moslehi J, Muller FL, Guo M, et al. Telomere dysfunction induces metabolic and mitochondrial compromise. Nature. 2011;470:359-65.

[15] Li FC, Yen JC, Chan SH, Chang AY. Bioenergetics failure and oxidative stress in brain stem mediates cardiovascular collapse associated with fatal methamphetamine intoxication. PLoS One. 2012;7:e30589.

[16] Shao D, Fry JL, Han J, Hou X, Pimentel DR, Matsui R, et al. A redox-resistant sirtuin-1 mutant protects against hepatic metabolic and oxidant stress. J Biol Chem. 2014;289:7293-306.

[17] Rider OJ, Francis JM, Ali MK, Holloway C, Pegg T, Robson MD, et al. Effects of catecholamine stress on diastolic function and myocardial energetics in obesity. Circulation. 2012;125:1511-9.

[18] Rider OJ, Francis JM, Tyler D, Byrne J, Clarke K, Neubauer S. Effects of weight loss on myocardial energetics and diastolic function in obesity. Int J Cardiovasc Imaging. 2013;29:1043-50.

[19] Wojtovich AP, Smith CO, Haynes CM, Nehrke KW, Brookes PS. Physiological consequences of complex II inhibition for aging, disease, and the mKATP channel. Biochim Biophys Acta. 2013;1827:598-611.

[20] Yankovskaya V, Horsefield R, Tornroth S, Luna-Chavez C, Miyoshi H, Leger C, et al. Architecture of succinate dehydrogenase and reactive oxygen species generation. Science. 2003;299:700-4.

[21] Chung HS, Wang SB, Venkatraman V, Murray CI, Van Eyk JE. Cysteine oxidative posttranslational modifications: emerging regulation in the cardiovascular system. Circ Res. 2013;112:382-92.

[22] Wang SB, Foster DB, Rucker J, O'Rourke B, Kass DA, Van Eyk JE. Redox regulation of mitochondrial ATP synthase: implications for cardiac resynchronization therapy. Circ Res. 2011;109:750-7.

[23] Schilling B, Murray J, Yoo CB, Row RH, Cusack MP, Capaldi RA, et al. Proteomic analysis of succinate dehydrogenase and ubiquinol-cytochrome c reductase (Complex II and III) isolated by immunoprecipitation from bovine and mouse heart mitochondria. Biochim Biophys Acta. 2006;1762:213-22.

[24] Chen YR, Chen CL, Pfeiffer DR, Zweier JL. Mitochondrial complex II in the post-ischemic heart: oxidative injury and the role of protein S-glutathionylation. J Biol Chem. 2007;282:32640-54.

[25] Werth MT, Cecchini G, Manodori A, Ackrell BA, Schroder I, Gunsalus RP, et al. Site-directed mutagenesis of conserved cysteine residues in Escherichia coli fumarate reductase: modification of the spectroscopic and electrochemical properties of the [2Fe-2S] cluster. Proc Natl Acad Sci U S A. 1990;87:8965-9.

[26] Kohr MJ, Sun J, Aponte A, Wang G, Gucek M, Murphy E, et al. Simultaneous measurement of protein oxidation and S-nitrosylation during preconditioning and ischemia/reperfusion injury with resin-assisted capture. Circ Res. 2011;108:418-26.

[27] Murray CI, Kane LA, Uhrigshardt H, Wang SB, Van Eyk JE. Site-mapping of in vitro S-nitrosation in cardiac mitochondria: implications for cardioprotection. Mol Cell Proteomics. 2011;10:M110 004721.

[28] Boudina S, Han YH, Pei S, Tidwell TJ, Henrie B, Tuinei J, et al. UCP3 regulates cardiac efficiency and mitochondrial coupling in high fat-fed mice but not in leptin-deficient mice. Diabetes. 2012;61:3260-9.

[29] Chen YR, Zweier JL. Cardiac mitochondria and reactive oxygen species generation. Circ Res. 2014;114:524-37.

[30] Shen X, Zheng S, Metreveli NS, Epstein PN. Protection of cardiac mitochondria by overexpression of MnSOD reduces diabetic cardiomyopathy. Diabetes. 2006;55:798-805.

[31] Janczewski AM, Lakatta EG. Modulation of sarcoplasmic reticulum Ca(2+) cycling in systolic and diastolic heart failure associated with aging. Heart Fail Rev. 2010;15:431-45.

Figure 1. Increased H_2O_2 production rate and decreased GSH/GSSG ratio in cardiac mitochondria from mice fed a HFHS vs. control diet. A) H_2O_2 production rate with a complex I substrate (5 mM pyruvate + 5mM malate); **B**) H_2O_2 production rate with a complex II substrate (5 mM succinate) and inhibition of reverse electron transport (2µM rotenone); **C**) Mitochondrial GSH/GSSG ratio; D) Whole tissue (LV) GSH/GSSG ratio. (n=4-5 per group)

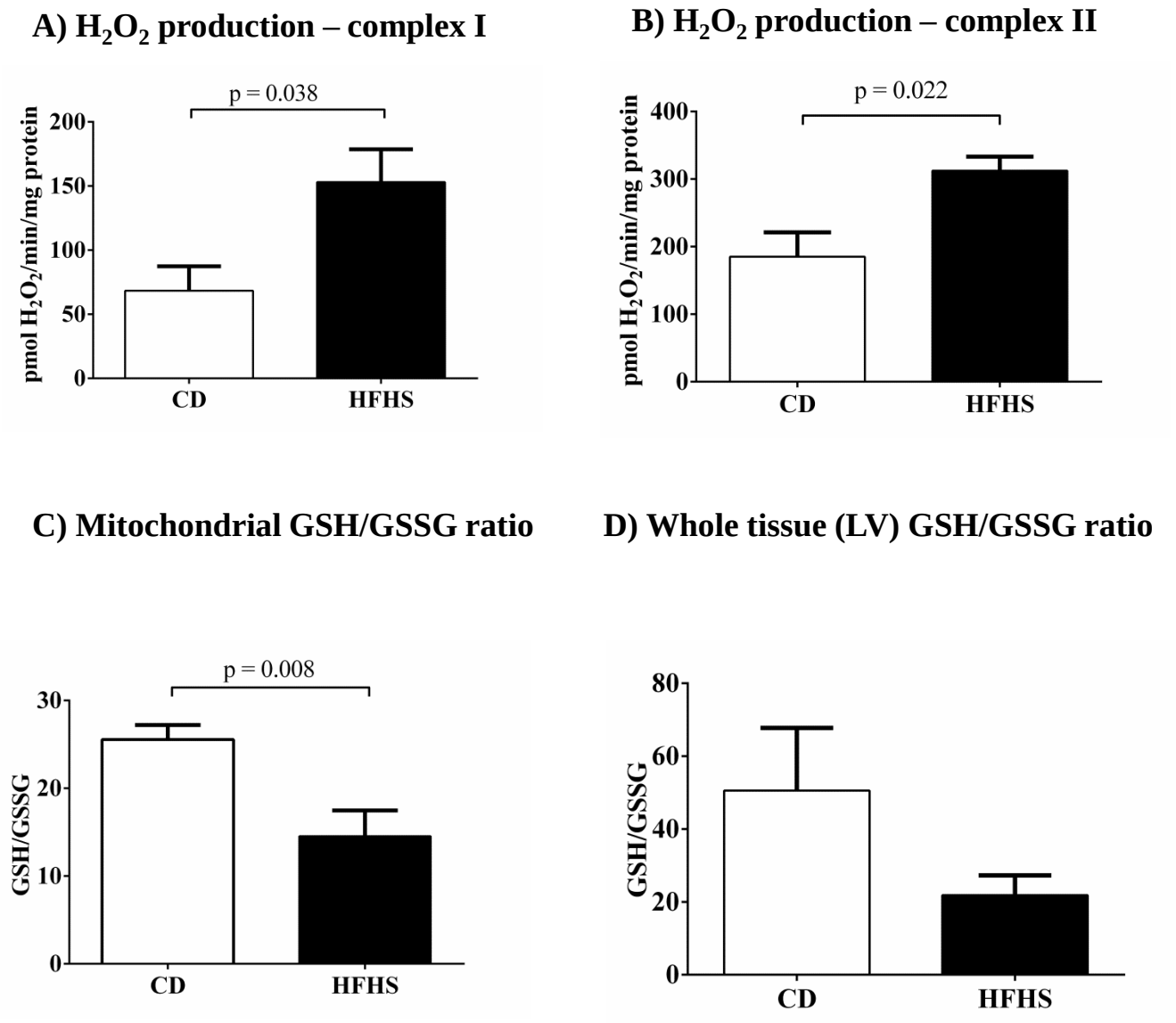

Figure 2. Decreased ATP synthesis rate and complex II activity in cardiac mitochondria from mice fed a HFHS vs. control diet, and effect of DTT (5 mM). A) Complex I substrate-driven ATP synthesis rate (5 mM pyruvate + 5mM malate); **B**) Complex II substrate-driven ATP synthesis rate (5 mM succinate + 2µM rotenone); **C**) Complex II activity assessed by the reduction of ubiquinone. (n=4-5 per group)

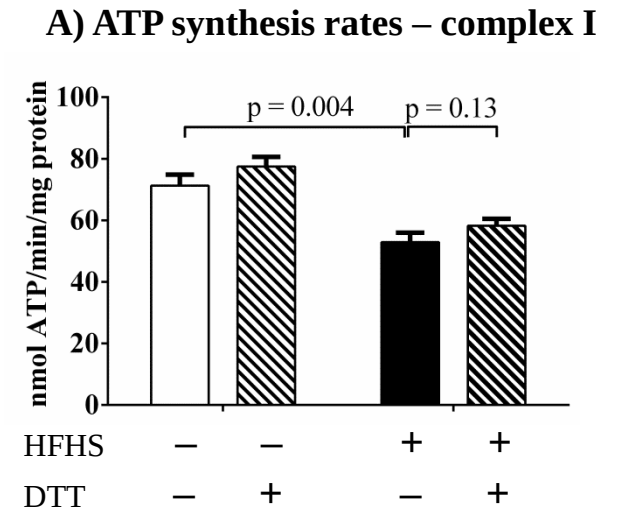

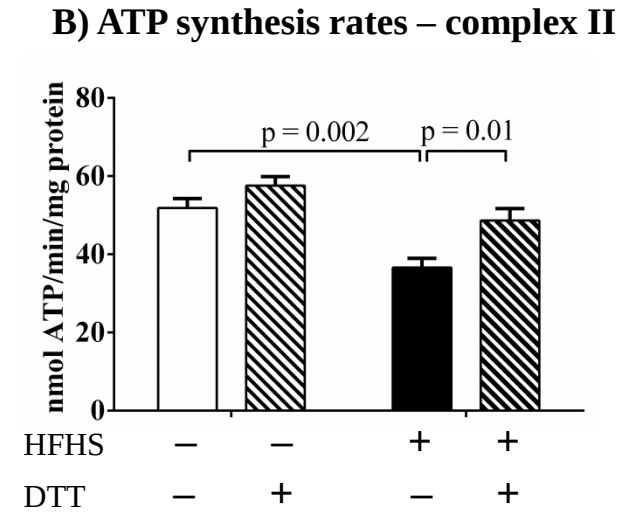

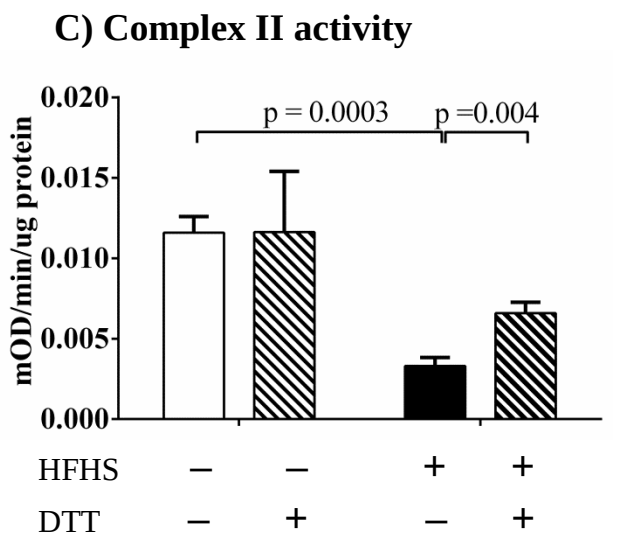

Figure 3. Biotin switch assay to detect reversibly-oxidized cysteines on SDHA and SDHB. A) Representative blots from biotin switch assay in which total represents protein labeled by the antibody for SDHA or SDHB, and BIAM represents the portion of total protein containing a reversible cysteine OPTM. **B** and **C**) Bar graphs showing the mean values for the ratio of BIAM-labeled to total protein, reflecting the proportion of reversibly-oxidized cysteines in SDHA (Panel **B**) or SDHB (Panel **C**). (n=3-4 per group) MW – molecular weight markers

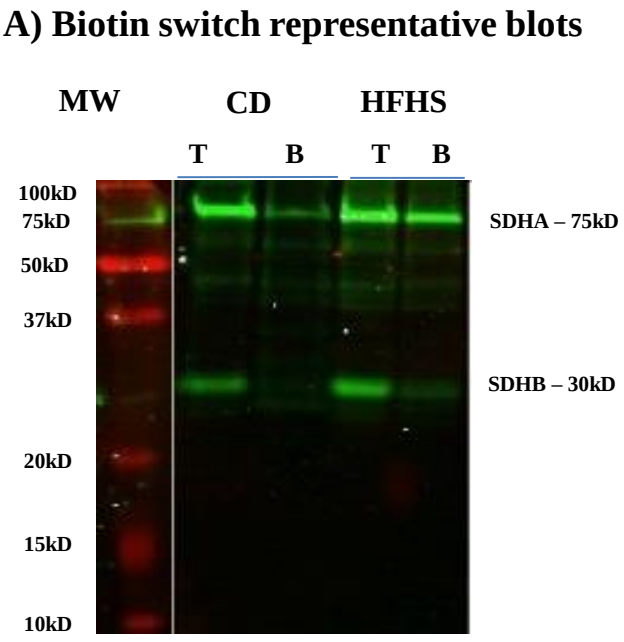

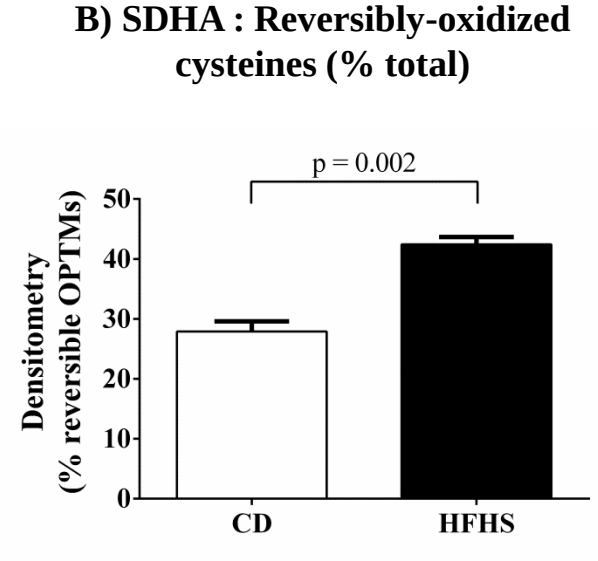

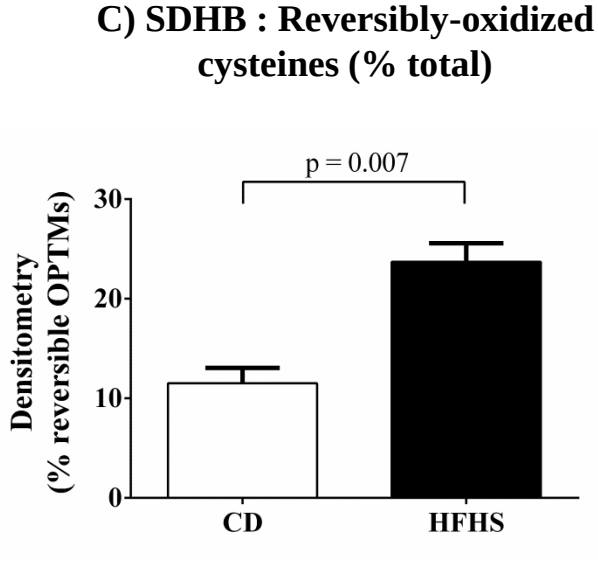

Figure 4. ETC protein and VDAC-1 expression. Expression of representative proteins the complexes of ETC (1 each from complex I, III, IV and V, and 2 from complex II). **A**) Representative Western blots. **B**) Mean values. VDAC-1 is indexed to GAPDH, and ETC proteins are indexed for VDAC-1 (n = 4 per group, p = ns for all). **S** – rat cardiac mitochondria control.

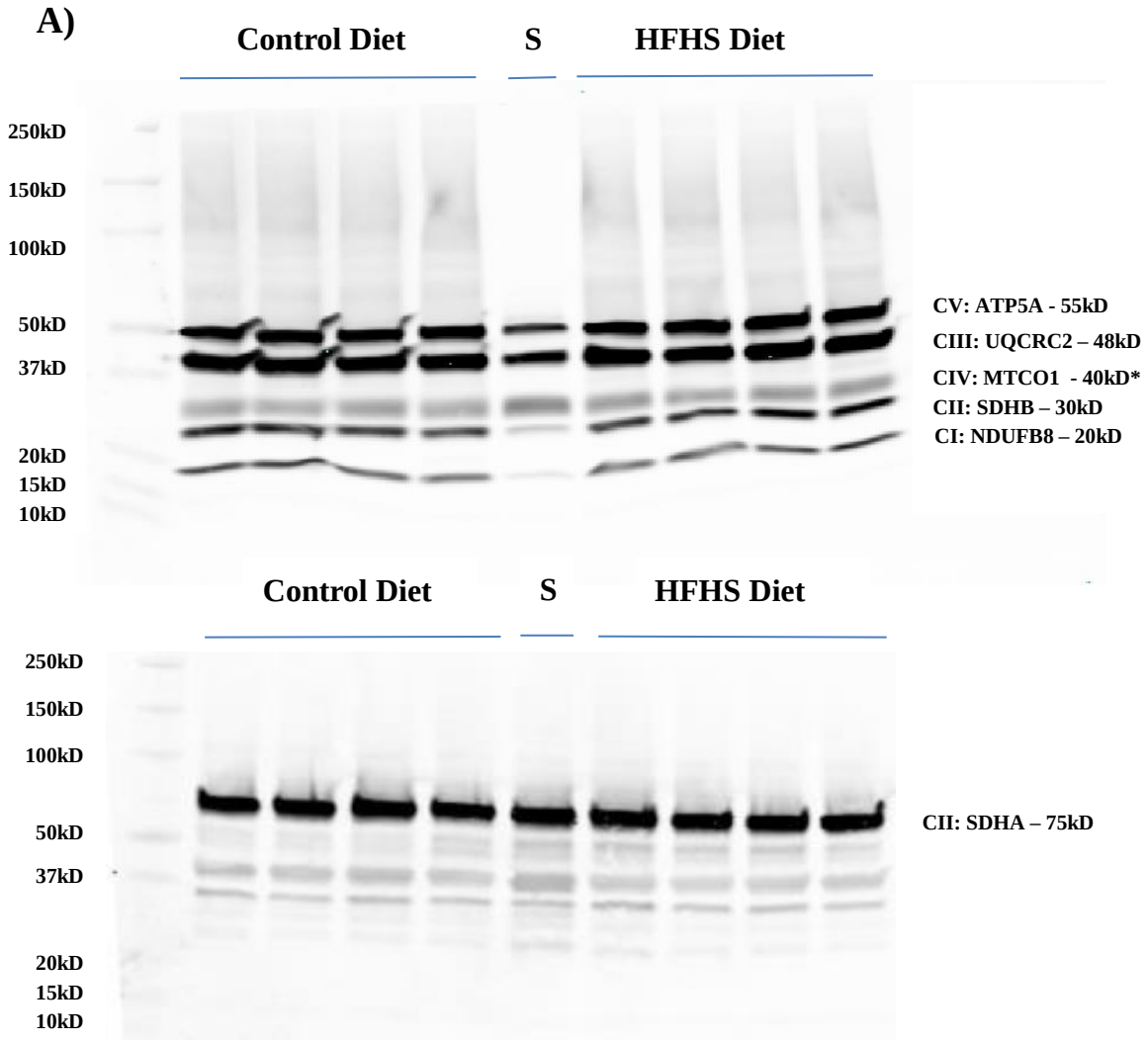

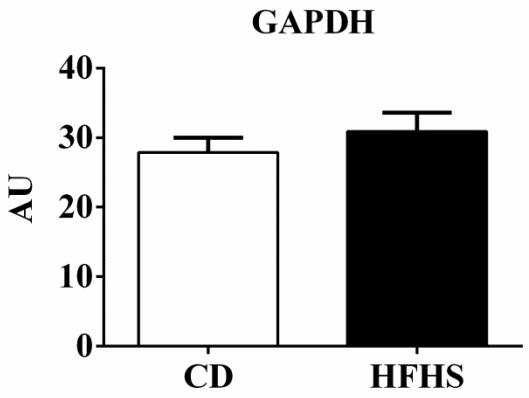
GAPDH
AU
40
30
20
10
0
CD
HFHS

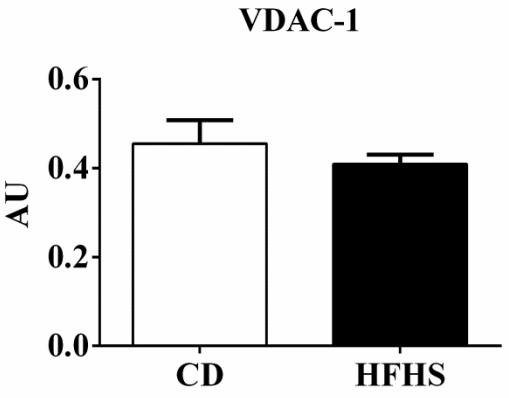
VDAC-1
AU
0.6
0.4
0.2
0.0
CD
HFHS

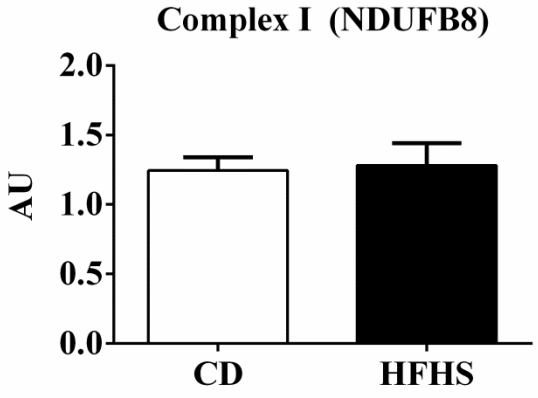
Complex I (NDUFB8)
AU
2.0
1.5
1.0
0.5
0.0
CD
HFHS

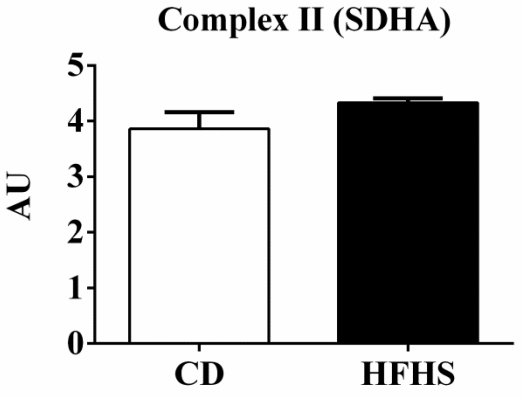
Complex II (SDHA)
AU
5
4
3
2
1
0
CD
HFHS

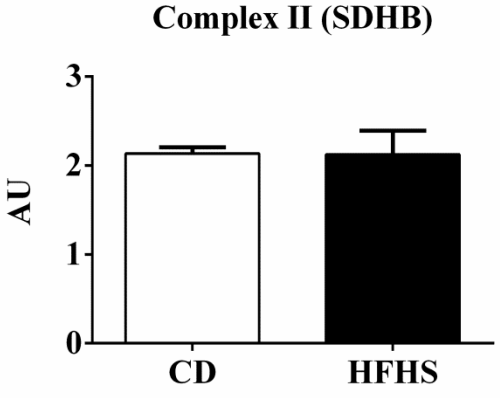
Complex II (SDHB)
AU
3
2
1
0
CD
HFHS

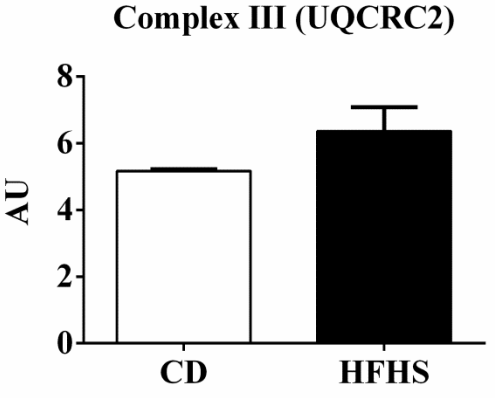
Complex III (UQCRC2)
AU
8
6
4
2
0
CD
HFHS

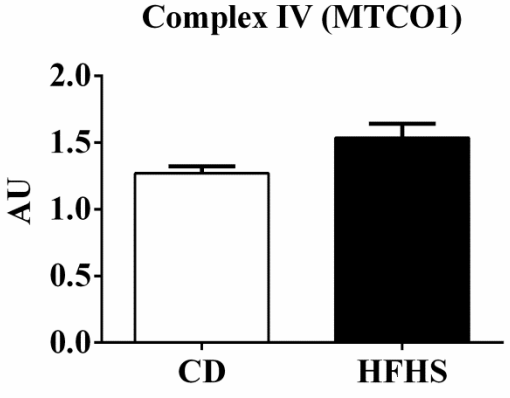
Complex IV (MTCO1)
AU
2.0
1.5
1.0
0.5
0.0
CD
HFHS

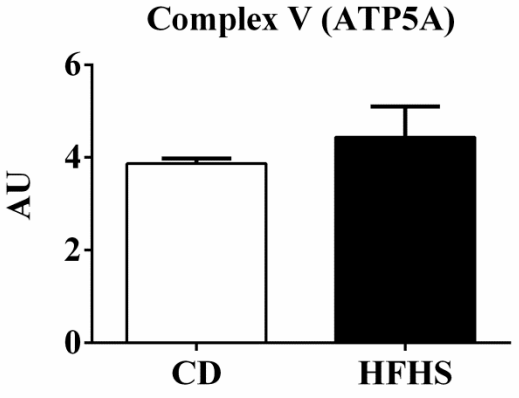
Complex V (ATP5A)
AU
6
4
2
0
CD
HFHS

Figure 5. Data analysis of reversible cysteine oxidation (representative example). A precursor ion from SDHA with mass-to-charge ratio (m/z) 677.35 was subjected to MS/MS in the Thermo Q Exactive Mass Spectrometer. Brackets within the peptide sequence indicate b (N-terminal) and y (C-terminal) fragment ions; their respective peaks are labeled in the MS/MS spectrum. Mascot software works backward from the fragment masses to identify the most likely sequence match, which in this case was AAFGLSEAGFNTA**c**LTK, or cys-89. For each identified cysteine, reporter ion masses were detected in the low mass region (m/z 126-129) of the tandem mass spectrum. The intensities of m/z 127 and 129 represent the magnitude of reversible cysteine OPTM (m/z) for Control and HFHS, respectively. Given unchanged protein expression (see Figure 4), we compared these ions directly. This particular cysteine was oxidized 1.94 in the HFHS-fed mice compared to control diet fed.

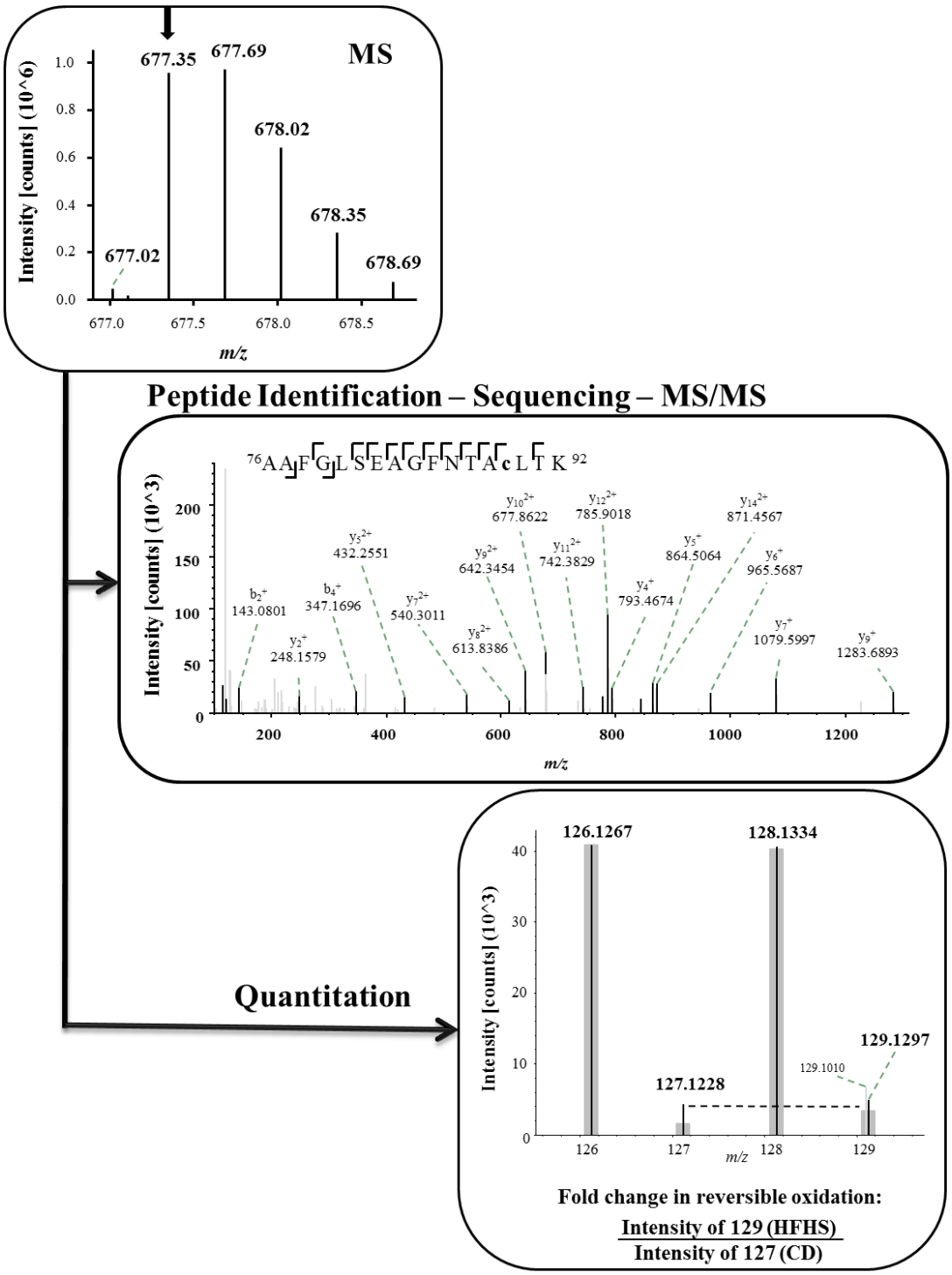

Supplemental Material

Table 1S. Composition of HFHS and control diets. D09071702 is HFHS diet and D09071703 is control diet.

	D09071702		D09071703	
Product #				
	gm%	kcal%	gm%	kcal%
Protein	20.5	15	15.0	15
Carbohydrate	38.2	28	76.3	75
Fat	35.5	58	4.5	10
Total		100.0		100.0
kcal/gm	5.54		4.05	
Ingredient	gm	kcal	gm	kcal
Casein	182	728	182	728
DL-Methionine	3	12	3	12
Maltodextrin 10	170	680	170	680
Corn starch	0	0	760	3040
Sucrose	164	656	0	0
Lard	320	2880	55	495
Salt Mix, S10026B	50	0	50	0
Vitamin Mix, V10001	10	40	10	40
Choline Bitartrate	2	0	2	0
Total	901	4996	1232.0	4995

Figure 1S. HFHS-fed mice develop progressive obesity starting at 2 months on diet.